# Exactly separable version of X(5) and related models

Dennis Bonatsos[a1], D. Lenis[a2], E. A. McCutchan[b3], D. Petrellis[a4], I. Yigitoglu[c5]

[a] Institute of Nuclear Physics, N.C.S.R. "Demokritos",
GR-15310 Aghia Paraskevi, Attiki, Greece
[b] Wright Nuclear Structure Laboratory, Yale University,
New Haven, Connecticut 06520-8124, USA
[c] Hasan Ali Yucel Faculty of Education, Istanbul University,
TR-34470 Beyazit, Istanbul, Turkey

**Abstract**

One-parameter exactly separable versions of the X(5) and X(5)-$\beta^2$ models, labelled as ES-X(5) and ES-X(5)-$\beta^2$ respectively, are derived by using in the Bohr Hamiltonian potentials of the form $u(\beta) + u(\gamma)/\beta^2$. Unlike X(5), in these models the $\beta_1$ and $\gamma_1$ bands are treated on equal footing. Spacings within the $\gamma_1$ band are well reproduced by both models, while spacings within the $\beta_1$ band are well reproduced only by ES-X(5)-$\beta^2$, for which several nuclei with $R_{4/2} = E(4_1^+)/E(2_1^+)$ ratios and [normalized to $E(2_1^+)$] $\beta_1$ and $\gamma_1$ bandheads corresponding to the model predictions have been found.

## 1 Introduction

The introduction of the X(5) critical point symmetry [1] has stirred considerable effort in studying related special solutions [2, 3, 4, 5] of the Bohr collective Hamiltonian [6], as well as in identifying nuclei exhibiting experimentally [7, 8] this behaviour, with considerable success. However, some open questions remain:

1) The separation of variables used in X(5) and related models is approximate. In particular, a potential of the form $u(\beta) + u(\gamma)$ is used, where $\beta$ and $\gamma$ are the usual collective variables [6]. In the X(5) model [1] an infinite square well potential is used as $u(\beta)$, while a harmonic oscillator potential centered around $\gamma = 0$ is used as $u(\gamma)$. In the X(5)-$\beta^2$ model [5] a harmonic oscillator potential, $\beta^2/2$, is used as $u(\beta)$. Separation of variables is based on two approximations: a) the limitation to small angles for $\gamma$, b) the replacement of $\beta^2$ by its average value $\langle\beta^2\rangle$ in the terms involved in the $\gamma$-equation. Exact numerical diagonalization of the Bohr Hamiltonian [9], carried out using a recently introduced computationally

[1]e-mail: bonat@inp.demokritos.gr
[2]e-mail: lenis@inp.demokritos.gr
[3]e-mail: elizabeth.ricard-mccutchan@yale.edu
[4]e-mail: petrellis@inp.demokritos.gr
[5]e-mail: yigitoglu@istanbul.edu.tr

tractable version [10, 11, 12] of the Bohr–Mottelson collective model [6], pointed out that the first approximation is valid for large $\gamma$ stiffness, while the second approximation is valid for small $\gamma$ stiffness.

2) X(5) [1] and the related X(5)-$\beta^2$ model [5] contain no free parameter (up to overall scale factors) in the ground state band and $\beta$ bands, but free parameters appear in the $\gamma$ bands and $K = 4$ bands. As a result the bandheads of the ground state band and the $\beta$ bands, as well as their internal structure, are fixed by the theory without any free parameter, while the bandheads of the $\gamma$ bands and $K = 4$ bands contain free parameters. It would have been preferable to treat the $\beta$ and $\gamma$ bands on equal footing [13].

In the present work we try to circumvent these problems by using potentials of the form $u(\beta) + u(\gamma)/\beta^2$, which are known to lead to exact separation of variables [14, 15, 16, 17]. Then the following modifications occur:

1) The second approximation (replacement of $\beta^2$ by $\langle\beta^2\rangle$) is avoided. The first approximation, namely the limitation to small angles for $\gamma$, is still used, in order to obtain simplified solutions of the $\gamma$ equation, but it can be a good one if stiffness is kept large [9], which indeed turns out to be the case when comparisons to experimental data are performed.

2) The models obtained in this way contain one free parameter in all bands, the stiffness of $\gamma$. As a result the relative position of all bandheads and the internal structure of all bands is fixed by the theory using one parameter, the $\beta_1$ and $\gamma_1$ bands treated on equal footing, as it is desirable [13].

Recent studies on critical point symmetries [1, 2, 3] have made clear that the relative position of bandheads in a nucleus, as well as the internal spacing in each band, are key structural features which should be reproduced by a model. The internal spacing of the $\beta_1$ and $\gamma_1$ bands, relative to that of the ground state band, will be shown to provide a stringent test for the various special solutions of the Bohr Hamiltonian.

The models occuring from the exact separation of variables will be described in Section 2, while in Section 3 some numerical results and comparisons to experiment will be given. Finally, a discussion of the present results and plans for further work will be given in Section 4.

# 2 Spectra

The original Bohr Hamiltonian [6] is

$$H = -\frac{\hbar^2}{2B}\left[\frac{1}{\beta^4}\frac{\partial}{\partial\beta}\beta^4\frac{\partial}{\partial\beta} + \frac{1}{\beta^2\sin 3\gamma}\frac{\partial}{\partial\gamma}\sin 3\gamma\frac{\partial}{\partial\gamma} - \frac{1}{4\beta^2}\sum_{k=1,2,3}\frac{Q_k^2}{\sin^2\left(\gamma - \frac{2}{3}\pi k\right)}\right] + V(\beta,\gamma), \tag{1}$$

where $\beta$ and $\gamma$ are the usual collective coordinates, while $Q_k$ ($k = 1, 2, 3$) are the components of angular momentum in the intrinsic frame, and $B$ is the mass parameter.

One seeks [1] solutions of the relevant Schrödinger equation having the form $\Psi(\beta,\gamma,\theta_i) = \phi_K^L(\beta,\gamma)\mathcal{D}^L_{M,K}(\theta_i)$, where $\theta_i$ ($i = 1, 2, 3$) are the Euler angles, $\mathcal{D}(\theta_i)$ denote Wigner functions of them, $L$ are the eigenvalues of angular momentum, while $M$ and $K$ are the eigenvalues of the projections of angular momentum on the laboratory-fixed $z$-axis and the body-fixed $z'$-axis respectively.

As pointed out in Ref. [1], in the case in which the potential has a minimum around $\gamma = 0$ one can write the angular momentum term of Eq. (1) in the form

$$\sum_{k=1,2,3} \frac{Q_k^2}{\sin^2\left(\gamma - \frac{2\pi}{3}k\right)} \approx \frac{4}{3}(Q_1^2 + Q_2^2 + Q_3^2) + Q_3^2\left(\frac{1}{\sin^2\gamma} - \frac{4}{3}\right). \tag{2}$$

Using this result in the Schrödinger equation corresponding to the Hamiltonian of Eq. (1), introducing [1] reduced energies $\epsilon = 2BE/\hbar^2$ and reduced potentials $u = 2BV/\hbar^2$, and assuming that the reduced potential can be separated into two terms of the form $u(\beta,\gamma) = u(\beta) + u(\gamma)/\beta^2$, as in Refs. [14, 15, 16, 17], the Schrödinger equation can be separated into two equations

$$\left[-\frac{1}{\beta^4}\frac{\partial}{\partial\beta}\beta^4\frac{\partial}{\partial\beta} + \frac{L(L+1)}{3\beta^2} + u(\beta) + \frac{\lambda}{\beta^2}\right]\xi_L(\beta) = \epsilon\xi_L(\beta), \tag{3}$$

$$\left[-\frac{1}{\sin 3\gamma}\frac{\partial}{\partial\gamma}\sin 3\gamma\frac{\partial}{\partial\gamma} + \frac{K^2}{4}\left(\frac{1}{\sin^2\gamma} - \frac{4}{3}\right) + u(\gamma)\right]\eta_K(\gamma) = \lambda\eta_K(\gamma). \tag{4}$$

Eq. (4) for $\gamma \approx 0$ can be treated as in Ref. [1], considering a potential of the form $u(\gamma) = (3c)^2\gamma^2/2$ and expanding in powers of $\gamma$. Then Eq. (4) takes the form

$$\left[-\frac{1}{\gamma}\frac{\partial}{\partial\gamma}\gamma\frac{\partial}{\partial\gamma} + \frac{K^2}{4\gamma^2} + (3c)^2\frac{\gamma^2}{2}\right]\eta_K(\gamma) = \epsilon_\gamma\eta_K(\gamma), \tag{5}$$

with $\epsilon_\gamma = \lambda + \frac{K^2}{3}$. The solution is given in terms of Laguerre polynomials [1]

$$\epsilon_\gamma = (3c)(n_\gamma + 1), \qquad n_\gamma = 0, 1, 2, \ldots, \tag{6}$$

$$n_\gamma = 0, \quad K = 0; \qquad n_\gamma = 1, \quad K = \pm 2; \qquad n_\gamma = 2, \quad K = 0, \pm 4; \qquad \ldots, \tag{7}$$

$$\eta_{n_\gamma,K}(\gamma) = C_{n,K}\gamma^{|K/2|}e^{-(3c)\gamma^2/2}L_n^{|K/2|}(3c\gamma^2), \qquad n = (n_\gamma - |K/2|)/2. \tag{8}$$

Eq. (3) is then solved exactly for the case in which $u(\beta)$ is an infinite well potential

$$u(\beta) = \begin{cases} 0 & \text{if } \beta \le \beta_W \\ \infty & \text{for } \beta > \beta_W \end{cases}. \tag{9}$$

Setting [1] $\tilde{\xi}(\beta) = \beta^{3/2}\xi(\beta)$, $\epsilon = k_\beta^2$, and $z = \beta k_\beta$, one obtains the Bessel equation

$$\frac{d^2\tilde{\xi}}{dz^2} + \frac{1}{z}\frac{d\tilde{\xi}}{dz} + \left[1 - \frac{\nu^2}{z^2}\right]\tilde{\xi} = 0, \tag{10}$$

with

$$\nu = \sqrt{\frac{L(L+1)-K^2}{3} + \frac{9}{4} + 3c(n_\gamma+1)}. \tag{11}$$

From the boundary condition $\tilde{\xi}(\beta_W) = 0$ the energy eigenvalues are then [1]

$$\epsilon_{\beta;s,L} = (k_{s,L})^2, \qquad k_{s,L} = \frac{x_{s,L}}{\beta_W}, \tag{12}$$

where $x_{s,L}$ is the $s$-th zero of the Bessel function $J_\nu(k_{s,L}\beta)$, while the relevant eigenfunctions are

$$\xi_{s,L}(\beta) = C_{s,L}\beta^{-3/2}J_\nu(k_{s,L}\beta), \tag{13}$$

where $C_{s,L}$ are normalization constants. For $K = 0$ one has $L = 0,\ 2,\ 4,\ \ldots$, while for $K \neq 0$ one obtains $L = K,\ K+1,\ K+2,\ \ldots$

The full wave function reads

$$\Psi(\beta,\gamma,\theta_i) = C_{s,L}\beta^{-3/2}J_\nu(k_{s,L}\beta)\eta_{n_\gamma,K}(\gamma)\mathcal{D}^L_{MK}(\theta_i), \tag{14}$$

and should be properly symmetrized [1]

$$\Psi(\beta,\gamma,\theta_i) = \frac{1}{\sqrt{2}}\left[\phi_{L,K}(\beta,\gamma)\mathcal{D}^L_{MK}(\theta_i) + (-1)^{L+K}\phi_{L,-K}\mathcal{D}^L_{M,-K}(\theta_i)\right]. \tag{15}$$

Bands occuring in this model, characterized by $(s,\ n_\gamma)$, include the ground state band $(1,0)$, the $\beta_1$-band $(2,0)$, the $\gamma_1$-band $(1,1)$, the first $K = 4$ band $(1,2)$. The relative position of all levels depends on the single parameter $c$. Therefore the main difference between the present model and X(5) is that in the present model all bands are fixed by the single parameter $c$, while in X(5) the ground state band and the other $n_\gamma = 0$ bands are fixed in a parameter-free way, but the bandheads of the $n_\gamma \neq 0$ bands depend on free parameters.

In Ref. [18] a variant of the X(5) model has been considered, in which during the separation of variables the term $K^2/3$ has been kept in the $\beta$-equation, while in Ref. [1] this term has been put in the $\gamma$-equation. This choice leads to different results (different expression for $\nu$, in particular) when the method of Refs. [1, 18] is followed, but it makes no difference in the present approach.

Eq. (3) is exactly soluble also in the case in which $u(\beta) = \beta^2/2$. In this case, which is analogous to the X(5)-$\beta^2$ model [5], the eigenfunctions are [19]

$$F^L_n(\beta) = \left[\frac{2n!}{\Gamma\left(n+a+\frac{5}{2}\right)}\right]^{1/2}\beta^a L_n^{a+\frac{3}{2}}(\beta^2)e^{-\beta^2/2}, \tag{16}$$

where $\Gamma(n)$ stands for the $\Gamma$-function, $L^a_n(z)$ denotes the Laguerre polynomials, and

$$a = -\frac{3}{2} + \sqrt{\frac{L(L+1)-K^2}{3} + \frac{9}{4} + 3c(n_\gamma+1)}, \tag{17}$$

while the energy eigenvalues are

$$E_{n,L} = 2n + a + \frac{5}{2} = 2n + 1 + \sqrt{\frac{L(L+1) - K^2}{3} + \frac{9}{4} + 3c(n_\gamma + 1)}, \qquad n = 0, 1, 2, \ldots \quad (18)$$

In the above, $n$ is the usual oscillator quantum number. A formal correspondence between the energy levels of the X(5) analogue and the present X(5)-$\beta^2$ analogue can be established through the relation

$$n = s - 1. \quad (19)$$

It should be remembered, however, that the origin of the two quantum numbers is different, $s$ labelling the order of a zero of a Bessel function and $n$ labelling the number of zeros of a Laguerre polynomial. In the present notation, the ground state band corresponds to $s = 1$ ($n = 0$). For the energy states the notation $E_{s,L} = E_{n+1,L}$ of Ref. [1] will be kept.

On the present approach the following general comments apply.

a) The use of a potential of the form $u(\beta) + u(\gamma)/\beta^2$, instead of a potential of the form $u(\beta) + u(\gamma)$ [as in X(5) and X(5)-$\beta^2$] leads to exact separation of variables instead of an approximate one [14, 15, 16, 17]. As a result, no $\beta^2$ factors appear in the $\gamma$-equation, and therefore the approximation of replacing $\beta^2$ by its average value, $\langle\beta^2\rangle$, used in X(5) and X(5)-$\beta^2$, is avoided. Exact numerical diagonalizations [9] of the Bohr Hamiltonian have demonstrated that this approximation is valid only for small $\gamma$ stiffness. This requirement is removed in the present case.

b) However, the treatment of the $\gamma$-equation in the present approach is based on the same approximation of small $\gamma$ angles also used in the X(5) and X(5)-$\beta^2$ models. The potential $(3c)^2\gamma^2/2$ used here is the lowest order approximation for small $\gamma$ to the potential $c^2(1 - \cos 3\gamma)$, which has also been used in Ref. [20]. It should be reminded that the dependence on $\cos 3\gamma$ results from the symmetry requirements [6] of the Bohr Hamiltonian, explicitly listed in Ref. [21]. A two-dimensional oscillator in $\gamma$, similar to the one obtained here, has also been obtained in Ref. [20] in the limit of large $\gamma$ stiffness (large $c$ in the present notation). The exact numerical diagonalizations of the Bohr Hamiltonian carried out in Ref. [9] consistently demonstrated that the small angle approximation for $\gamma$ is good for large $\gamma$ stiffness, which in the present models can be achieved, since the requirement of small $\gamma$ stiffness is not present any more, as discussed in point a). In Sec. 3 we shall see that experimental data are reproduced for values of $c$ of order 10, corresponding to $(3c)^2 \approx 900$.

c) Small oscillations in $\gamma$ around the zero value, corresponding to axially deformed prolate shapes, have also been considered in Ref. [22], leading to the conclusion that $K$ can be considered as a good quantum number either if $\gamma$ is fixed to zero, or if the nucleus is strongly deformed. In Sec. 3 we shall see that good agreement with experimental data is obtained for nuclei with $R_{4/2} = E(4_1^+)/E(2_1^+) > 3.15$, i.e. for nuclei which are well deformed.

# 3 Numerical results and comparison to experiment

Numerical results for the present models, referred to as *exactly separable X(5)* [ES-X(5)] and *exactly separable X(5)-$\beta^2$* [ES-X(5)-$\beta^2$] respectively, are shown in Table 1, together with results for several other models, including X(5) [1], exact numerical diagonalization of the Bohr Hamiltonian [9] (labelled by "Caprio"), X(5)-$\beta^{2n}$ ($n = 1, 2, 3, 4$) [5], X(5) with a Davidson potential

$$u(\beta) = \beta^2 + \frac{\beta_0^4}{\beta^2}, \tag{20}$$

where $\beta_0$ is the minimum of the potential [4], labelled as X(5)-D. The collective quantities reported in Table 1 include the ground state band ratio $R_{4/2} = E(4_1^+)/E(2_1^+)$, the bandheads of the $\beta_1$ and $\gamma_1$ bands, $E(0_\beta^+)$ and $E(2_\gamma^+)$, normalized to $E(2_1^+)$, the spacings within the $\beta_1$ band relative to these of the ground state band

$$R_{2,0,\beta,g} = \frac{E(2_\beta^+) - E(0_\beta^+)}{E(2_1^+)}, \qquad R_{4,2,\beta,g} = \frac{E(4_\beta^+) - E(2_\beta^+)}{E(4_1^+) - E(2_1^+)}, \tag{21}$$

and the spacing within the $\gamma_1$ band relative to that of the ground state band

$$R_{4,2,\gamma,g} = \frac{E(4_\gamma^+) - E(2_\gamma^+)}{E(4_1^+) - E(2_1^+)}. \tag{22}$$

Experimental values for the energy ratios $R_{2,0,\beta,g}$, $R_{4,2,\beta,g}$, and $R_{4,2,\gamma,g}$ are shown in Fig. 1 for all nuclei with $A > 50$ (excluding magic and semimagic nuclei). The following comments can be made:

1) From Fig. 1(a),(b) it is clear that the majority of nuclei exhibit ratios $R_{2,0,\beta,g}$ and $R_{4,2,\beta,g}$ close to 1 or slightly below it, indicating that the spacings within the $\beta_1$ band are similar to the spacings within the ground state band, as expected for a band displaced from the ground state band by one quantum of $\beta$ vibration. Ratios exactly equal to 1 are provided by the X(5)-$\beta^2$, ES-X(5)-$\beta^2$, and X(5)-D models, guaranteed by the $\beta^2$ term present in the relevant potentials. X(5) gives values of 1.8 and 1.7 respectively, the well known point of disagreement with experimental ratios by a factor close to 2 [7, 8]. The exact numerical diagonalization of Ref. [9] provides similar or higher values, while ES-X(5) gives values around 1.5 . The X(5)-$\beta^4$, X(5)-$\beta^6$, and X(5)-$\beta^8$ models interpolate between X(5)-$\beta^2$ and X(5), as expected, since higher powers of $\beta^{2n}$ closer approximate the infinite well potential.

2) The above observations can be understood in the following way. It is known that the problem of overprediction of the spacing within the $\beta_1$ band by X(5) can be resolved by replacing the infinite well potential in $\beta$ by a potential with sloped walls [2]. The combination of the five-dimensional centrifugal term with the sloped well provides a potential with a minimum, resembling the Davidson potential of Eq. (20) as well as the sum of a harmonic oscillator potential and a centrifugal term.

3) From Fig. 1(c) it is clear that the majority of nuclei exhibit ratios $R_{4,2,\gamma,g}$ close to 1, indicating that the spacings within the $\gamma_1$ band are similar to the spacings within the ground state band. Among the models of Table 1, X(5), X(5)-$\beta^{2n}$, as well as X(5)-D, provide values slightly higher than 1, the ES-X(5) and ES-X(5)-$\beta^2$ models give values slightly lower than 1, while the exact numerical diagonalization of Ref. [9] is in between. It is interesting that in the X(5)-D model for large parameter values, the spacing within the $\gamma_1$ band becomes the same as within the ground state band and the $\beta_1$ bands, as expected in the SU(3) limit.

From the above observations it is expected that the one-parameter ES-X(5)-$\beta^2$ and X(5)-D models, as well as X(5)-$\beta^2$, are more appropriate for reproducing the correct spacings within the $\beta_1$ and $\gamma_1$ bands. However, the position of the bandheads is also important. It is then reasonable to look for nuclei for which a model can closely reproduce the $R_{4/2}$ ratio, characterizing the development of the ground state band, but also the development of the $\beta_1$ and $\gamma_1$ bands, according to the systematics of Fig. 1, as well as the normalized bandheads $E(0^+_\beta)/E(2^+_1)$ and $E(2^+_\gamma)/E(2^+_1)$. A search of all even nuclei with $Z > 50$, for which sufficient data exist [23], provided the results shown in Table 2. 18 examples have been found for ES-X(5)-$\beta^2$, as well as 4 examples for ES-X(5).

The basic difference between ES-X(5)-$\beta^2$ and ES-X(5) is shown in Table 3, where the ground state, $\beta_1$ and $\gamma_1$ bands of $^{156}$Gd, a good example of ES-X(5)-$\beta^2$, and $^{162}$Dy, a good example of ES-X(5), are shown. In the first case the agreement between theory and experiment remains good in all three bands up to high angular momenta, while in the second case this holds only for the ground state and $\gamma_1$ bands, the theoretical $\beta_1$ band diverging from the data with increasing angular momentum.

A final remark concerning the physical content of the models developed here, based on the potential of the form $u(\beta) + u(\gamma)/\beta^2$ [14, 15, 16, 17]. As already remarked in Ref. [14], one expects $\gamma$ stability to increase with deformation. This is corroborated by the results shown in Table 2, where it is clear that $c$ is increasing with $R_{4/2}$, indicating that $u(\gamma)$ is becoming more and more steep with increasing deformation, restricting the nucleus to $\gamma$ values very close to zero. As a result, the present models are applicable to strongly deformed nuclei close to axial symmetry.

# 4 Discussion

In summary, exactly separable one-parameter versions of the X(5) and X(5)-$\beta^2$ models, labelled as ES-X(5) and ES-X(5)-$\beta^2$, have been derived, by using potentials of the form $u(\beta) + u(\gamma)/\beta^2$. Unlike X(5), in these models the $\beta_1$ and $\gamma_1$ bands are treated on equal footing. The spacings within the $\gamma_1$ band are in agreement to experimental evidence in both models, while the spacings within the $\beta_1$ band are reproduced correctly only by ES-X(5)-$\beta^2$. Several nuclei for which the $R_{4/2}$ ratio, as well as the normalized positions of the $\beta_1$ and $\gamma_1$ bandheads are closely reproduced by ES-X(5)-$\beta^2$ have been identified. A detailed study of the complete level schemes of these nuclei, including B(E2) transition rates, is deferred to a longer publication.

# References


[1] F. Iachello, Phys. Rev. Lett. 87 (2001) 052502.

[2] M. A. Caprio, Phys. Rev. C 69 (2004) 044307.

[3] N. Pietralla, O. M. Gorbachenko, Phys. Rev. C 70 (2004) 011304.

[4] D. Bonatsos, D. Lenis, N. Minkov, D. Petrellis, P. P. Raychev, P. A. Terziev, Phys. Lett. B 584 (2004) 40.

[5] D. Bonatsos, D. Lenis, N. Minkov, P. P. Raychev, P. A. Terziev, Phys. Rev. C 69 (2004) 014302.

[6] A. Bohr, Mat. Fys. Medd. K. Dan. Vidensk. Selsk. 26 (1952) no. 14.

[7] R. F. Casten, N. V. Zamfir, Phys. Rev. Lett. 87 (2001) 052503.

[8] R. Krücken, et al., Phys. Rev. Lett. 88 (2002) 232501.

[9] M. A. Caprio, Phys. Rev. C 72 (2005) 054323.

[10] D. J. Rowe, Nucl. Phys. A 735 (2004) 372.

[11] D. J. Rowe, P. S. Turner, J. Repka, J. Math. Phys. 45 (2004) 2761.

[12] D. J. Rowe, P. S. Turner, Nucl. Phys. A 753 (2005) 94.

[13] F. Iachello, in G. Lo Bianco (Ed.), Symmetries and Low-Energy Phase Transition in Nuclear-Structure Physics, U. Camerino (2006) 1.

[14] L. Wilets and M. Jean, Phys. Rev. 102, 788 (1956).

[15] L. Fortunato, Eur. Phys. J. A 26, s01 (2005) 1.

[16] L. Fortunato, Phys. Rev. C 70 (2004) 011302.

[17] L. Fortunato, S. De Baerdemacker, and K. Heyde, Phys. Rev. C 74, 014310 (2006).

[18] R. Bijker, R. F. Casten, N. V. Zamfir, E. A. McCutchan, Phys. Rev. C 68 (2003) 064304.

[19] M. Moshinsky, J. Math. Phys. 25 (1984) 1555.

[20] M. Jean, Nucl. Phys. 21 (1960) 142.

[21] T. M. Corrigan, F. J. Margetan, S. A. Williams, Phys. Rev. C 14 (1976) 2279.

[22] A. S. Davydov, Nucl. Phys. 24 (1961) 682.

[23] Nuclear Data Sheets, as of December 2005.

## Figures

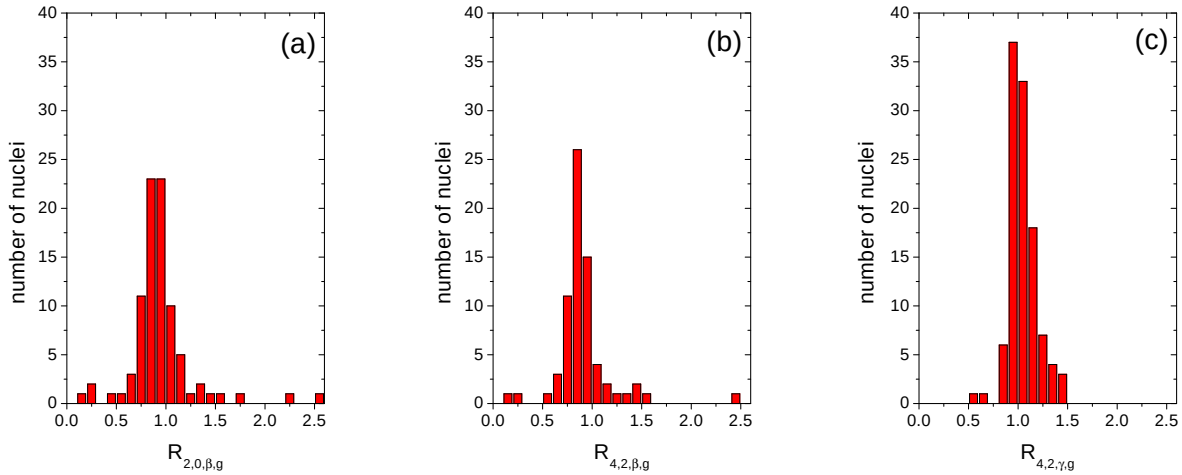


Figure 1: Experimental data for the energy ratios $R_{2,0,\beta,g}$ [Eq. (21)] (a), $R_{4,2,\beta,g}$ [Eq. (21)] (b), and $R_{4,2,\gamma,g}$ [Eq. (22)] (c). For each ratio, all nuclei with $A > 50$ (excluding magic and semimagic nuclei) for which sufficient experimental data (taken from Ref. [23]) exist, have been taken into account.

Table 1: The key collective quantities $R_{4/2} = E(4_1^+)/E(2_1^+)$, normalized $\beta_1$ bandhead $E(0_\beta^+)/E(2_1^+)$ (labelled as $0_\beta^+/2_1^+$), normalized $\gamma_1$ bandhead $E(2_\gamma^+)/E(2_1^+)$ (labelled as $2_\gamma^+/2_1^+$), spacings of the $\beta_1$ band relative to the ground state band $R_{2,0,\beta,g}$ [Eq. (21)] and $R_{4,2,\beta,g}$ [Eq. (21)], as well as spacing of the $\gamma_1$ band relative to the ground state band $R_{4,2\gamma,g}$ [Eq. (22)] are listed for different models, including X(5)-$\beta^{2n}$ [5], X(5) [1], X(5)-D [4], Caprio's exact numerical diagonalization of the Bohr Hamiltonian [9], and the present exactly separable analogues of X(5) [ES-X(5)] and X(5)-$\beta^2$ [ES-X(5)-$\beta^2$]. Parameter values, if present, are listed in the column "Par", using the definition and symbol of the relevant original publication. The notation "par" indicates that the corresponding quantity depends on an additional free parameter.

| model | Par | $R_{4/2}$ | $0_\beta^+/2_1^+$ | $2_\gamma^+/2_1^+$ | $R_{2,0,\beta,g}$ | $R_{4,2,\beta,g}$ | $R_{4,2,\gamma,g}$ |
|---|---|---|---|---|---|---|---|
| X(5)-$\beta^2$ | | 2.646 | 3.562 | par | 1.000 | 1.000 | 1.132 |
| X(5)-$\beta^4$ | | 2.769 | 4.352 | par | 1.250 | 1.205 | 1.101 |
| X(5)-$\beta^6$ | | 2.824 | 4.816 | par | 1.416 | 1.344 | 1.089 |
| X(5)-$\beta^8$ | | 2.852 | 5.091 | par | 1.528 | 1.441 | 1.083 |
| X(5) | | 2.904 | 5.649 | par | 1.801 | 1.701 | 1.071 |
| X(5)-D | $\beta_0$ | | | | | | |
| | 0.0 | 2.646 | 3.562 | par | 1.000 | 1.000 | 1.131 |
| | 1.0 | 2.756 | 4.094 | par | 1.000 | 1.000 | 1.108 |
| | 1.5 | 2.978 | 5.756 | par | 1.000 | 1.000 | 1.064 |
| | 2.0 | 3.156 | 8.772 | par | 1.000 | 1.000 | 1.031 |
| | 5.0 | 3.327 | 50.130 | par | 1.000 | 1.000 | 1.001 |
| Caprio | a | | | | | | |
| | 0. | 2.20 | 3.03 | 2.20 | 1.77 | 0.31 | 1.16 |
| | 200. | 2.76 | 5.66 | 6.09 | 2.31 | 1.74 | 1.15 |
| | 400. | 3.02 | 8.37 | 10.12 | 2.19 | 1.76 | 1.04 |
| | 600. | 3.12 | 10.26 | 13.42 | 2.00 | 1.79 | 0.95 |
| | 800. | 3.17 | 11.71 | 16.19 | 1.91 | 1.70 | 1.00 |
| | 1000. | 3.20 | 12.89 | 18.66 | 1.84 | 1.69 | 0.97 |
| ES-X(5) | c | | | | | | |
| | 2.0 | 3.166 | 10.298 | 3.166 | 1.649 | 1.606 | 0.929 |
| | 4.0 | 3.234 | 13.643 | 5.955 | 1.579 | 1.552 | 0.909 |
| | 6.0 | 3.264 | 16.451 | 8.764 | 1.534 | 1.515 | 0.904 |
| | 8.3 | 3.283 | 19.292 | 12.013 | 1.497 | 1.484 | 0.903 |
| | 10.0 | 3.292 | 21.210 | 14.423 | 1.477 | 1.465 | 0.904 |
| | 12.0 | 3.299 | 23.317 | 17.266 | 1.456 | 1.447 | 0.905 |
| | 13.7 | 3.304 | 25.012 | 19.692 | 1.442 | 1.433 | 0.906 |
| ES-X(5)-$\beta^2$ | c | | | | | | |
| | 2.0 | 3.006 | 6.074 | 3.006 | 1.000 | 1.000 | 0.852 |
| | 4.0 | 3.117 | 7.806 | 5.516 | 1.000 | 1.000 | 0.796 |
| | 6.0 | 3.171 | 9.217 | 8.011 | 1.000 | 1.000 | 0.771 |
| | 8.0 | 3.204 | 10.439 | 10.502 | 1.000 | 1.000 | 0.757 |
| | 10.0 | 3.225 | 11.531 | 12.991 | 1.000 | 1.000 | 0.749 |
| | 12.0 | 3.241 | 12.529 | 15.478 | 1.000 | 1.000 | 0.742 |
| | 14.0 | 3.252 | 13.453 | 17.965 | 1.000 | 1.000 | 0.738 |

Table 2: Comparison of theoretical predictions of the exactly separable analogue of the X(5)-$\beta^2$ model [ES-X(5)-$\beta^2$] (upper part) and of the exactly separable analogue of the X(5) model [ES-X(5)] (lower part) to experimental $R_{4/2} = E(4_1^+)/E(2_1^+)$ ratios, as well as to experimental $\beta_1$ and $\gamma_1$ bandheads, normalized to the $2_1^+$ state and labelled by $0_\beta^+/2_1^+$ and $2_\gamma^+/2_1^+$ respectively. All data have been taken from Ref. [23].

| nucleus | $R_{4/2}$ exp | $0_\beta^+/2_1^+$ exp | $2_\gamma^+/2_1^+$ exp | $c$ | $R_{4/2}$ th | $0_\beta^+/2_1^+$ th | $2_\gamma^+/2_1^+$ th |
|---|---|---|---|---|---|---|---|
| $^{188}$Os | 3.083 | 7.008 | 4.083 | 2.9 | 3.068 | 6.908 | 4.139 |
| $^{186}$Os | 3.165 | 7.736 | 5.596 | 4.0 | 3.117 | 7.806 | 5.516 |
| $^{184}$Os | 3.203 | 8.698 | 7.870 | 5.7 | 3.165 | 9.019 | 7.637 |
| $^{184}$W | 3.274 | 9.014 | 8.122 | 6.0 | 3.171 | 9.217 | 8.011 |
| $^{162}$Er | 3.230 | 10.654 | 8.827 | 7.0 | 3.189 | 9.847 | 9.257 |
| $^{166}$Yb | 3.228 | 10.189 | 9.108 | 7.0 | 3.189 | 9.847 | 9.257 |
| $^{158}$Dy | 3.206 | 10.014 | 9.567 | 7.3 | 3.194 | 10.028 | 9.630 |
| $^{170}$Er | 3.310 | 11.335 | 11.883 | 9.2 | 3.218 | 11.107 | 11.995 |
| $^{182}$W | 3.291 | 11.346 | 12.201 | 9.4 | 3.220 | 11.215 | 12.244 |
| $^{180}$Hf | 3.307 | 11.807 | 12.855 | 10.0 | 3.225 | 11.531 | 12.991 |
| $^{156}$Gd | 3.239 | 11.796 | 12.972 | 10.0 | 3.225 | 11.531 | 12.991 |
| $^{228}$Ra | 3.207 | 11.300 | 13.258 | 10.1 | 3.226 | 11.583 | 13.115 |
| $^{170}$Yb | 3.293 | 12.692 | 13.598 | 10.7 | 3.231 | 11.890 | 13.861 |
| $^{230}$Th | 3.273 | 11.934 | 14.687 | 11.3 | 3.236 | 12.189 | 14.608 |
| $^{228}$Th | 3.235 | 14.402 | 16.776 | 13.4 | 3.249 | 13.182 | 17.219 |
| $^{154}$Sm | 3.254 | 13.410 | 17.567 | 13.7 | 3.251 | 13.318 | 17.592 |
| $^{172}$Yb | 3.305 | 13.245 | 18.616 | 14.4 | 3.254 | 13.630 | 18.463 |
| $^{232}$U | 3.291 | 14.530 | 18.221 | 14.5 | 3.255 | 13.674 | 18.587 |
| $^{166}$Er | 3.289 | 18.118 | 9.754 | 6.7 | 3.271 | 17.352 | 9.751 |
| $^{162}$Dy | 3.294 | 17.332 | 11.011 | 7.6 | 3.278 | 18.462 | 11.022 |
| $^{162}$Gd | 3.291 | 19.792 | 11.983 | 8.3 | 3.283 | 19.292 | 12.013 |
| $^{176}$Yb | 3.308 | 21.661 | 15.352 | 10.6 | 3.294 | 21.857 | 15.275 |

Table 3: Comparison of the predictions of the exactly separable analogue of the X(5)-$\beta^2$ model [ES-X(5)-$\beta^2$] (with $c = 10.0$) to the experimental spectrum of $^{156}$Gd [23] (upper part), and of the predictions of the exactly separable analogue of X(5) [ES-X(5)] (with $c = 7.6$) to the experimental spectrum of $^{162}$Dy [23] (lower part). The energy levels of the ground state band (gsb), the $\beta_1$ band, and the $\gamma_1$ band are normalized to the $2_1^+$ level.

| | | gsb | gsb | $\beta_1$ | $\beta_1$ | | $\gamma_1$ | $\gamma_1$ |
|---|---|---|---|---|---|---|---|---|
| | L | exp | th | exp | th | L | exp | th |
| $^{156}$Gd | | | | | | | | |
| | 0 | 0.000 | 0.000 | 11.796 | 11.531 | 2 | 12.972 | 12.991 |
| | 2 | 1.000 | 1.000 | 12.695 | 12.531 | 3 | 14.027 | 13.712 |
| | 4 | 3.239 | 3.225 | 14.587 | 14.757 | 4 | 15.235 | 14.656 |
| | 6 | 6.573 | 6.468 | 17.311 | 17.999 | 5 | 16.937 | 15.811 |
| | 8 | 10.848 | 10.500 | 20.775 | 22.031 | 6 | 18.474 | 17.162 |
| | 10 | 15.916 | 15.122 | 24.952 | 26.653 | 7 | 20.792 | 18.692 |
| | 12 | 21.631 | 20.179 | 30.435 | 31.710 | 8 | 22.607 | 20.388 |
| | 14 | 27.828 | 25.559 | | | 9 | 25.285 | 22.233 |
| | 16 | 34.388 | 31.180 | | | 10 | 27.452 | 24.213 |
| $^{162}$Dy | | | | | | | | |
| | 0 | 0.000 | 0.000 | 17.332 | 18.462 | 2 | 11.011 | 11.022 |
| | 2 | 1.000 | 1.000 | 18.020 | 19.969 | 3 | 11.938 | 11.909 |
| | 4 | 3.294 | 3.278 | 19.518 | 23.369 | 4 | 13.154 | 13.081 |
| | 6 | 6.800 | 6.733 | 21.913 | 28.445 | 5 | 14.664 | 14.532 |
| | 8 | 11.412 | 11.259 | 24.619 | 34.975 | 6 | 16.420 | 16.255 |
| | 10 | 17.044 | 16.768 | 28.041 | 42.778 | 7 | 18.477 | 18.242 |
| | 12 | 23.572 | 23.195 | 32.156 | 51.721 | 8 | 20.709 | 20.485 |
| | 14 | 30.895 | 30.493 | 36.640 | 61.705 | 9 | 23.284 | 22.975 |
| | 16 | 38.904 | 38.625 | | | 10 | 25.879 | 25.708 |
| | 18 | 47.583 | 47.568 | | | 11 | 28.981 | 28.676 |
| | | | | | | 12 | 31.396 | 31.873 |
| | | | | | | 13 | 35.453 | 35.295 |
| | | | | | | 14 | 39.437 | 38.936 |